https://doi.org/10.5194/acp-2022-595
Preprint. Discussion started: 23 August 2022

Atmospheric Chemistry and Physics Discussions

Aqueous SOA formation from photosensitized guaiacol oxidation: Comparison between non-phenolic and phenolic methoxybenzaldehydes as photosensitizers in the absence and presence of ammonium nitrate

Beatrix Rosette Go Mabato[1,2], Yong Jie Li[3], Dan Dan Huang[4], Yalin Wang[3], and Chak K. Chan[1,2]*

[1]School of Energy and Environment, City University of Hong Kong, Hong Kong, China
[2]City University of Hong Kong Shenzhen Research Institute, Shenzhen, China
[3]Department of Civil and Environmental Engineering, and Centre for Regional Ocean, Faculty of Science and Technology, University of Macau, Macau, China
[4]Shanghai Academy of Environmental Sciences, Shanghai 200233, China

Correspondence to: Chak K. Chan (Chak.K.Chan@cityu.edu.hk)

Abstract. Aromatic carbonyls (e.g., methoxybenzaldehydes), an important class of photosensitizers, are abundant in the atmosphere. This study compared non-phenolic (3,4-dimethoxybenzaldehyde, DMB) and phenolic (vanillin, VL) methoxybenzaldehydes as photosensitizers for aqueous secondary organic aerosol (aqSOA) formation via guaiacol (GUA) oxidation under atmospherically relevant cloud and fog conditions. The effects of ammonium nitrate (AN) on these reactions were also explored. GUA oxidation by triplet excited states of DMB (^{3}DMB*) (GUA+DMB) was ~4 times faster and exhibited greater light absorption than oxidation by ^{3}VL* (GUA+VL). Both GUA+DMB and GUA+VL formed aqSOA composed of oligomers, functionalized monomers, oxygenated ring-opening species, and N-containing products in the presence of AN. The observation of N-heterocycles such as imidazoles indicates the participation of ammonium in the reactions. The majority of generated aqSOA are potential brown carbon (BrC) chromophores. Oligomerization and functionalization dominated in GUA+DMB and GUA+VL, but functionalization appeared to be more important in GUA+VL due to contributions from VL itself. AN did not significantly affect the oxidation kinetics, but it had distinct effects on the product distributions, likely due to differences in the photosensitizing abilities and structural features of DMB and VL. In particular, the more extensive fragmentation in GUA+DMB than in GUA+VL likely generated more N-containing products in GUA+DMB+AN. In GUA+VL+AN, the increased oligomers may be due to VL-derived phenoxy radicals induced by $^{\bullet}OH$ or $^{\bullet}NO_2$ from nitrate photolysis. Furthermore, increased nitrated products observed in the presence of both DMB or VL and AN than in AN alone implies that photosensitized reactions may promote nitration. This work demonstrates how the structural features of photosensitizers affect aqSOA formation via non-carbonyl phenol oxidation. Potential interactions between photosensitization and AN photolysis were also elucidated. These findings facilitate a better

https://doi.org/10.5194/acp-2022-595
Preprint. Discussion started: 23 August 2022

Atmospheric Chemistry and Physics Discussions

understanding of photosensitized aqSOA formation and highlight the importance of ammonium nitrate photolysis in these reactions.

1 Introduction

Photosensitized reactions involving triplet excited states of organic compounds ($^3C^*$) are efficient pathways for the formation of secondary organic aerosol in the aqueous phase (aqSOA; Smith et al., 2014, 2016; Yu et al., 2014, 2016; Chen et al., 2020; Jiang et al., 2021; Misovich et al., 2021; Mabato et al., 2022). Upon irradiation by solar radiation, photosensitizers form an excited triplet state that directly reacts with substrates (e.g., phenols), and can generate singlet oxygen ($^1O_2$), superoxide ($O_2^{\bullet-}$) or hydroperoxyl ($^{\bullet}HO_2$) radicals, and hydroxyl radicals ($^{\bullet}OH$) upon reactions with O_2 and substrates (George et al., 2018; Chen et al., 2020), thereby facilitating the oxidation of rather volatile species and contributing to aqSOA formation. An important class of photosensitizers is aromatic carbonyls (e.g., methoxybenzaldehydes) which are abundant in aerosol particles, cloud waters, and fog waters (Anastasio et al., 1997; Felber et al., 2021). Aromatic carbonyls can be emitted from anthropogenic sources and biomass burning (BB; Lipari et al.,1984; Edye and Richards, 1991; Hawthorne et al., 1992; Simoneit et al., 1993, 1999; Anastasio et al., 1997; Felber et al., 2021), or formed via atmospheric oxidation of aromatic hydrocarbons (Hoshino et al., 1978; Calvert and Madronich, 1987; Anastasio et al., 1997; Felber et al., 2021). BB is also a significant source of phenols through lignin pyrolysis (Simpson et al., 2005). Phenolic carbonyls have a hydroxyl (–OH) group on the aromatic ring, whereas non-phenolic carbonyls do not. BB smoke has been reported to have comparable concentrations of phenolic and non-phenolic carbonyls (Simoneit et al., 1993; Anastasio et al., 1997).

Most previous studies on aqSOA formation via photosensitized non-carbonyl phenol oxidation have examined 3,4-dimethoxybenzaldehyde (DMB), a non-phenolic methoxybenzaldehyde, as the photosensitizer (Smith et al., 2014, 2015; Yu et al., 2014, 2016; Chen et al., 2020; Jiang et al., 2021; Misovich et al., 2021). By contrast, phenolic carbonyls have been mainly studied as aqSOA precursors via $^{\bullet}OH$-, nitrate-, nitrite-, and ^{3}DMB*-mediated oxidation (Li et al., 2014; Huang et al., 2018; Pang et al., 2019; Jiang et al., 2021; Misovich et al., 2021). However, strongly light-absorbing phenolic carbonyls (e.g., molar absorptivity above 300 nm $\geq 7 \times 10^3$ M^{-1} cm^{-1}) can also serve as photosensitizers to promote aqSOA formation (Smith et al., 2016; Mabato et al., 2022). For instance, the direct photosensitized oxidation of phenolic carbonyls (i.e., oxidation of phenolic carbonyls by their $^3C^*$ or $^3C^*$-derived oxidants) such as vanillin (VL; another methoxybenzaldehyde) efficiently form low-volatility products, with aqSOA mass yields of up to 140% (Smith et al., 2016). Moreover, the aqSOA mass yields from the oxidation of syringol by ^{3}DMB* and ^{3}VL* are similar (111% and 114%, respectively; Smith et al., 2014, 2016). In addition, we recently reported that the direct photosensitized oxidation of VL and guaiacol oxidation by ^{3}VL* yield similar products (oligomers, functionalized monomers, and oxygenated ring-opening products) as observed with ^{3}DMB* (Yu et al., 2014; Mabato et al., 2022). Guaiacol is a non-carbonyl BB methoxyphenol with an emission rate from fireplace wood combustion in the range of 172 to 279 mg/kg (Schauer et al., 2001; Simoneit, 2002). The atmospheric

https://doi.org/10.5194/acp-2022-595
Preprint. Discussion started: 23 August 2022

Atmospheric Chemistry and Physics Discussions

reactivity of methoxyphenols has recently been reviewed (Liu et al., 2022). However, our experiments were performed at a concentration (0.1 mM VL) higher than what was typically used for DMB (0.005 to 0.01 mM; Smith et al., 2014, 2015; Yu et al., 2014, 2016). Therefore, direct comparisons between photosensitization by ^{3}DMB* and ^{3}VL* cannot be made. Despite the above findings, much is still unknown about how aqSOA formation proceeds in systems using phenolic carbonyls as photosensitizers.

BB aerosols are typically internally mixed with other aerosol components, such as ammonium nitrate (AN; Zielinski et al., 2020). Hence, aromatic carbonyls and phenols may coexist with AN in BB aerosols. Nitrate and ammonium facilitate the formation of aqSOA and brown carbon (BrC) via a number of pathways. Nitrate photolysis can produce $^{\bullet}$OH and nitrating agents (e.g., $^{\bullet}NO_2$; Minero et al., 2007; Huang et al., 2018; Mabato et al., 2022; Wang et al., 2022; Yang et al., 2022), and ammonium reacts with carbonyls to yield N-containing heterocycles (e.g., imidazoles) and oligomers capable of UV-Vis light absorption (De Haan et al., 2009, 2011; Nozière et al., 2009, 2010, 2018; Shapiro et al., 2009; Yu et al., 2011; Lee et al., 2013; Powelson et al., 2014; Gen et al., 2018; Grace et al., 2019; Mabato et al., 2019). Furthermore, nitrate photolysis may be an important process for SO_2 oxidation and SOA formation in the particle phase (Gen et al., 2019a, 2019b, 2022; Zhang et al., 2020, 2021, 2022), and it can potentially modify the morphology of atmospheric viscous particles (Liang et al., 2021). Yet, understanding of the effects of inorganic nitrate on aqSOA formation remains limited. In addition, aqSOA formation studies involving aromatic carbonyls and phenols have probed either photosensitization or nitrate-mediated photo-oxidation, but these reactions can occur simultaneously. For instance, we previously reported nitrated compounds, including a potential imidazole derivative from the direct photosensitized oxidation of VL in the presence of AN (Mabato et al., 2022). Accordingly, investigations on reaction systems including both photosensitizers and AN may provide further insights into the aqueous-phase processing of BB aerosols.

In this work, we compared aqSOA formation from photosensitized guaiacol (GUA) oxidation by ^{3}C* of non-phenolic and phenolic methoxybenzaldehydes under identical conditions (simulated sunlight and concentration) relevant to cloud and fog waters. The effects of AN on photosensitized aqSOA formation were also examined. In this study, the dominant aqSOA precursor is GUA (Henry's law constant of 9.2×10^2 M atm^{-1}; Sagebiel et al., 1992), and DMB and VL were used as photosensitizers to oxidize GUA. DMB and VL (Henry's law constants of 5.4×10^1 M atm^{-1} and 4.7×10^5 M atm^{-1}, respectively; Yaws, 1994; EPI Suite version 4.1, 2012; Felber et al., 2021), which are also abundant in BB emissions (Schauer et al., 2001; Li et al., 2014; Chen et al., 2017; Pang et al., 2019; Mabato et al., 2022) and whose structures differ only by one functional group (–OCH_3 for the former and –OH for the latter, Fig. 1), represented non-phenolic and phenolic methoxybenzaldehydes, respectively. The structures of GUA, DMB, and VL are provided in Figure 1. Based on their quantum yield of ^{3}C* formation, DMB and VL have been classified as moderate and poor photosensitizers, respectively (Felber et al., 2021). The photosensitized oxidation of GUA by ^{3}DMB* or ^{3}VL* in the absence (and presence) of AN are referred to as GUA+DMB(+AN) and GUA+VL(+AN), respectively. GUA photo-oxidation by AN alone (GUA+AN) was also explored for comparison with GUA+DMB+AN and GUA+VL+AN. The molar absorptivities of GUA, DMB, VL, and

https://doi.org/10.5194/acp-2022-595
Preprint. Discussion started: 23 August 2022


Atmospheric Chemistry and Physics Discussions

nitrate are shown in Figure 1. The precursor and photosensitizer decay kinetics, detected products, and absorbance enhancement were used to characterize the reactions.

While several studies on photo-oxidation of BB emissions are available, this work focuses on the comparison between non-phenolic and phenolic methoxybenzaldehydes as photosensitizers in the absence and presence of AN for aqSOA formation. We found that GUA oxidation by ^{3}DMB* was faster and exhibited greater light absorption relative to GUA+VL. These are likely attributed to the stronger photosensitizing ability of DMB and the –OH group of VL, making it more prone to oxidation and more reactive towards electrophilic aromatic substitution. Oligomerization and functionalization dominated in GUA+DMB and GUA+VL, but functionalization appeared to be more significant in GUA+VL due to VL transformation products. Although AN did not significantly influence the oxidation kinetics due to the predominant role of photosensitizer chemistry compared to nitrate, AN promoted the formation of N-containing products. These include N-heterocycles (e.g., imidazoles), suggesting the participation of ammonium in the reactions. Moreover, the product distributions indicate distinct interactions between photosensitization by ^{3}DMB* and ^{3}VL* and AN photolysis. In particular, AN generated more N-containing products in GUA+DMB+AN and increased the oligomers in GUA+VL+AN. Furthermore, increased nitrated compounds in GUA+DMB+AN and GUA+VL+AN compared to GUA+AN suggest that photosensitized reactions may promote reactions by nitrate photolysis.

2 Methods

2.1 Aqueous phase photo-oxidation experiments

Procedures for the photo-oxidation experiments are presented in detail in our previous study (Mabato et al., 2022). Experimental solutions were prepared using 0.1 mM guaiacol (GUA, Sigma Aldrich, ≥98.0%) and 0.01 mM 3,4-dimethoxybenzaldehyde (DMB, Acros Organics, 99+%) or 0.01 mM vanillin (VL, Acros Organics, 99%, pure), in the absence and presence of ammonium nitrate (1 mM; AN, Acros Organics, 99+%, for analysis). These GUA and methoxybenzaldehydes concentrations are within the values expected in cloud or fog drops in areas with significant wood combustion (Anastasio et al., 1997; Rogge et al., 1998; Nolte et al., 2001). The AN concentration represents values usually observed in cloud and fog waters (Munger et al., 1983; Collett et al., 1998; Zhang and Anastasio, 2003; Li et al., 2011; Giulianelli et al., 2014; Bianco et al., 2020). It must be noted that this study did not intend to identify the AN concentrations that would affect the kinetics but attempted to analyze the effects of AN on photosensitized aqSOA formation. A solution composed of 0.1 mM GUA and 1 mM AN (GUA+AN) was also examined for comparison with GUA+DMB+AN and GUA+VL+AN. Sulfuric acid (H_2SO_4; Acros Organics, ACS reagent, 95% solution in water) was used to adjust the pH of the solutions to 4, which is within typical cloud pH values (2–7; Pye et al., 2020) and pH values observed in wood burning-impacted cloud and fog waters (Collett et al., 1998; Raja et al., 2008). The solutions were bubbled with synthetic air for 30 min before irradiation and throughout the reactions to achieve air-saturated conditions (Du et al., 2011; Chen et al., 2020) and were continuously magnetically stirred. In this study, the reactions can generate ^{3}DMB*/^{3}VL* and secondary oxidants

https://doi.org/10.5194/acp-2022-595
Preprint. Discussion started: 23 August 2022

Atmospheric Chemistry and Physics Discussions

($^1O_2$, $O_2^{\bullet-}$/$^\bullet HO_2$, $^\bullet OH$) but not ozone. Solutions contained in a quartz photoreactor were irradiated using a xenon lamp (model 6258, Ozone free xenon lamp, 300 W, Newport) equipped with a longpass filter (20CGA-305 nm cut-on filter, Newport) to eliminate light below 300 nm. The reaction temperatures were maintained at 27 ± 2 °C using cooling fans positioned around the photoreactor and lamp housing. The averaged initial photon flux in the reactor measured from 300 to 380 nm was ~3 × 10^{15} photons cm^{-2} s^{-1} nm^{-1} (Fig. 1), similar to our previous work (Mabato et al., 2022). Samples were collected every 30 mins for 180 mins for offline analyses of (1) GUA, DMB, and VL concentrations using ultra-high-performance liquid chromatography with photodiode array detector (UHPLC-PDA); (2) reaction products using UHPLC coupled with heated electrospray ionization Orbitrap mass spectrometry (UHPLC-HESI-Orbitrap-MS) operated in positive and negative ion modes; (3) concentrations of small organic acids using ion chromatography (IC); and (4) absorbance measurements using UV-Vis spectrophotometry. Each experiment was repeated independently at least three times. The reported decay rate constants, small organic acids concentration, and absorbance enhancement were averaged from triplicate experiments, and the corresponding errors represent one standard deviation. The pseudo-first-order rate constant (*k'*) for GUA decay was determined using the following equation (Huang et al., 2018):

$$ln\left([\mathrm{GUA}]_t/[\mathrm{GUA}]_0\right) = -k't \quad \text{(Eq. 1)}$$

where $[GUA]_t$ and $[GUA]_0$ are GUA concentrations at time *t* and 0, respectively. DMB or VL decay rate constants were calculated by replacing GUA with DMB or VL in Eq. 1. The decay rate constants were normalized to the photon flux measured for each experiment through dividing *k'* by the measured 2-nitrobenzaldehyde (2NB; a chemical actinometer) decay rate constant, *j*(2NB) (Mabato et al., 2022). Moreover, two independently prepared samples for each reaction condition were analyzed using UHPLC-HESI-Orbitrap-MS. Only peaks that were reproducibly detected in both sets of samples were considered. For clarity, the formulas discussed in this work correspond to neutral analytes (e.g., with H^+ or NH_4^+ removed from the ion formula). The details of the analytical procedures are provided in the Supplement (Sects. S1 to S4).

2.2 Calculation of the normalized abundance of products

The normalized abundance of products ([P], unitless) was introduced in our previous work (Mabato et al., 2022). Briefly, equal ionization efficiencies of different compounds, which is commonly used to estimate O:C ratios of SOA (Bateman et al., 2012; Lin et al., 2012; Laskin et al., 2014; De Haan et al., 2019) was assumed for the calculation:

$$[\mathrm{P}] = \frac{\mathrm{A}_{P,t}}{\mathrm{A}_{GUA,t}} \cdot \frac{[\mathrm{GUA}]_t}{[\mathrm{GUA}]_0} \quad \text{(Eq. 2)}$$

where $A_{P,t}$ and $A_{GUA,t}$ are the extracted ion chromatogram (EIC) peak areas of the product P and GUA from UHPLC-HESI-Orbitrap-MS analyses at time *t*, respectively; $[GUA]_t$ and $[GUA]_0$ are the GUA concentrations (μM) determined using UHPLC-PDA at time *t* and 0, respectively. Note that the normalized abundance of products has intrinsic uncertainties due to the variability in ionization efficiencies for various compounds. Nevertheless, it is a semi-quantitative analysis that gives an

https://doi.org/10.5194/acp-2022-595
Preprint. Discussion started: 23 August 2022


Atmospheric Chemistry and Physics Discussions

overview of how the signal intensities changed under different experimental conditions but not the quantification of the absolute product concentration.

3 Results and Discussion

Using kinetics data, MS analyses, and absorbance enhancement data, we first examined the differences between GUA+DMB and GUA+VL (Sect. 3.1). Then, we analyzed GUA+DMB+AN, GUA+VL+AN, and GUA+AN (Sect. 3.2) to explore the effects of nitrate photolysis and ammonium on photosensitized aqSOA formation.

3.1 Comparison of photosensitized GUA oxidation by non-phenolic (^{3}DMB*) and phenolic (^{3}VL*) methoxybenzaldehydes

Prior studies have reported that photosensitized non-carbonyl phenol oxidation in the presence of 3,4-dimethoxybenzaldehyde (DMB) and vanillin (VL) (separately) was mainly driven by ^{3}DMB* and ^{3}VL*, respectively (Smith et al., 2014; Mabato et al., 2022), while contributions from secondary oxidants such as $^1O_2$ and $^{\bullet}$OH were likely minor. However, both ^{3}DMB* and ^{3}VL* are efficiently quenched by O_2, suggesting that energy transfer should be considered in evaluating photosensitized processes involving these methoxybenzaldehydes (Felber et al., 2021). Moreover, it was found that ^{3}DMB*, $^1O_2$, and $O_2^{\bullet-}$ were the major contributors to the photosensitized oxidation of 4-ethylguaiacol (Chen et al., 2020). Recently, the oxidation of guaiacyl acetone (a non-conjugated phenolic carbonyl) in the presence of DMB has been reported to be initiated by ^{3}DMB*, $^1O_2$, $^{\bullet}$OH, or methoxy radical ($^{\bullet}OCH_3$) (Misovich et al., 2021). Further studies are thus required to identify the specific oxidants in these reaction systems. In this study, reactions initiated in the presence of DMB or VL are collectively referred to as photosensitized reactions. The reaction conditions, initial guaiacol (GUA) and DMB or VL decay rate constants, normalized product abundance, and the chemical characteristics of aqSOA formed in this work are summarized in Table 1.

3.1.1 Kinetic analysis of photosensitization by ^{3}DMB* and ^{3}VL*

No significant loss of GUA or photosensitizers was observed for dark experiments. Upon irradiation, the GUA decay rate constant in GUA+DMB was ~4 times higher than in GUA+VL. In GUA+DMB, the decay rate constant of GUA was ~8 times higher than that of DMB, consistent with a previous study (Smith et al., 2014). Contrastingly, the decay rate constant of VL was 2.4 times higher than that of GUA in GUA+VL. This VL consumption was also observed in our earlier work using 0.1 mM GUA + 0.1 mM VL (Mabato et al., 2022). These trends could be explained by the following reasons. First, DMB has a stronger photosensitizing ability than VL based on its higher quantum yield of ^{3}C* formation and longer lifetime of ^{3}DMB* compared to ^{3}VL* (Felber et al., 2021). Second, VL is also a phenolic compound similar to GUA, and is therefore highly reactive towards oxidation. For instance, its –OH group can be oxidized by ^{3}VL* via H-atom abstraction to form phenoxy radicals which can undergo coupling to form oligomers (Kobayashi and Higashimura, 2003; Sun et al., 2010;

https://doi.org/10.5194/acp-2022-595
Preprint. Discussion started: 23 August 2022


Atmospheric Chemistry and Physics Discussions

Mabato et al., 2022). The faster consumption of VL than GUA suggests a competition between ground-state VL and GUA for reaction with ^{3}VL*. Moreover, compared to a –OCH_3 group (in DMB), an –OH group (in VL) has a stronger electron-donating ability and is thus more activating. Relative to DMB, VL is more reactive towards electrophilic addition of •OH and electrophilic aromatic substitution.

3.1.2 Product distributions and chemical characteristics of aqSOA from photosensitization by ^{3}DMB* and ^{3}VL*

The products detected using UHPLC-HESI-Orbitrap-MS were used to represent the aqSOA formed in this work. The signal-weighted distributions of aqSOA calculated from combined positive (POS) and negative (NEG) ion modes MS results are summarized in Figure 2. The signal-weighted distributions calculated separately from POS and NEG ion modes MS results are available in Figures S1 and S2. Oligomers and derivatives of GUA dominated both GUA+DMB and GUA+VL, in agreement with pronounced oligomerization from triplet-mediated oxidation of relatively high phenol concentration (e.g., 0.1 to 3 mM; Li et al., 2014; Yu et al., 2014, 2016; Slikboer et al., 2015; Ye et al., 2019; Mabato et al., 2022). GUA+DMB had a higher oligomer contribution than GUA+VL, attributable to faster GUA oxidation by ^{3}DMB*. Figure 3 schematically depicts the main differences between photosensitized GUA oxidation by ^{3}DMB* and ^{3}VL* in the absence and presence of AN. As shown in Fig. 3, ^{3}DMB* and ^{3}VL* can oxidize GUA via H-atom abstraction to form phenoxy radicals which undergo coupling to form oligomers (Kobayashi and Higashimura, 2003; Sun et al., 2010; Mabato et al., 2022). The higher oligomer contribution in GUA+DMB is likely due to the better photosensitizing ability of DMB than VL and partly the lower abundance of ^{3}VL* due to fast VL consumption. VL was consumed faster than DMB during GUA oxidation ascribable to the –OH group of VL, making it more susceptible to oxidation and more reactive towards electrophilic aromatic substitution. In addition, the normalized product abundance for GUA+DMB was ~4 times higher than that for GUA+VL (Table 1), further suggesting more efficient photosensitized GUA oxidation by ^{3}DMB* than by ^{3}VL*. The oxidation of GUA or transient organic intermediates by secondary oxidants (e.g., $^1O_2$ and •OH) from ^{3}DMB* or ^{3}VL* and the fragmentation of larger compounds generate highly oxidized ring-opening products (Yu et al., 2014; Huang et al., 2018; Chen et al., 2020). GUA+DMB had a higher contribution of ring-opening products than GUA+VL, likely due to the greater availability of secondary oxidants in the former and fast VL consumption lowering the production of these species in GUA+VL. The IC analyses also indicate the formation of small organic acids (e.g., formic acid), which appeared to have higher concentrations in the presence of DMB than in VL (Fig. S3). The reactions of secondary oxidants or ring-opening products with GUA can form functionalized products. Notably, the contribution of monomers in GUA+VL was almost twice as high as in GUA+DMB, ascribable to VL transformation products. We previously showed that for the direct photosensitized oxidation of VL, functionalization prevails over oligomerization at 0.01 mM VL, the [VL] used in this work, while oligomerization dominates at higher [VL] (0.1 mM; Mabato et al., 2022).

It has been reported that oligomerization could occur during the electrospray ionization process (Yasmeen et al., 2010). In this work, it was confirmed that the oligomers observed were generated in the solutions via aqueous reactions

https://doi.org/10.5194/acp-2022-595
Preprint. Discussion started: 23 August 2022


Atmospheric Chemistry and Physics Discussions

instead of being artefacts of HESI-MS. This is based on the absence of dimers and higher oligomers in the HESI mass spectra of dark control solutions acquired by direct infusion (Yu et al., 2016).

The major GUA+DMB and GUA+VL products (Tables S1-S2) are mostly oligomers which can be formed through the coupling of phenoxy radicals (Kobayashi and Higashimura, 2003; Sun et al., 2010; Mabato et al., 2022). GUA+DMB products matched those reported in previous works on ^{3}DMB*- and/or $^{\bullet}$OH-mediated phenol oxidation (Yu et al., 2014, 2016). These include GUA dimers and trimers (e.g., $C_{14}H_{14}O_4$ and $C_{21}H_{18}O_8$, #1 and 19; Table S1), aldehydes ($C_7H_6O_4$, #13; Table S1), and esters ($C_{16}H_{18}O_6$, #14; Table S1). Functionalized products include $C_{11}H_{12}O_5$ and $C_{10}H_{12}O_3$ (#8 and 12; Table S1). More than half of the major GUA+VL products are the same oligomers detected from GUA+DMB (e.g., $C_{13}H_{10}O_4$ and $C_{20}H_{18}O_6$, #4 and 21; Table S1). The rest are mainly functionalized species such as $C_7H_8O_4$ and $C_8H_8O_5$ (#28 and 35; Table S2), corresponding to a hydroxylated GUA and hydroxylated VL, respectively.

The average elemental ratios and elemental distribution of the products (Fig. S4a–d) were consistent with those in previous studies on similar reaction systems (Yu et al., 2014, 2016; Mabato et al., 2022). The majority of the GUA+DMB and GUA+VL products had H:C ≤1.0 and O:C ≤0.5, typical for aromatic species (Mazzoleni et al., 2012; Kourtchev et al., 2014; Jiang et al., 2021). GUA+DMB had more compounds with higher O:C (≥0.6), in agreement with higher contributions of ring-opening products than in GUA+VL (Fig. 2). The higher $\langle OS_C \rangle$ for GUA+VL than in GUA+DMB (Table 1) was probably due to the significant functionalization in the former. Moreover, the distributions of OS_C and carbon number (Fig. S5a–d) show that these aqSOA products have similar elemental composition to those of low-volatility oxygenated organic aerosols (LV-OOA), semi-volatile oxygenated organic aerosols (SV-OOA), and slightly with biomass burning organic aerosols (BBOA) (Kroll et al., 2011). Further discussions on van Krevelen diagrams (Fig. S4a–d) and OS_C vs carbon number plots (Fig. S5a–d) for GUA+DMB and GUA+VL aqSOA are available in the Supplement (Sect. S5). In brief, ^{3}DMB*-initiated GUA oxidation was faster and yielded higher normalized product abundance than oxidation by ^{3}VL*. This is likely due to the stronger photosensitizing ability of DMB than VL and the –OH group of VL facilitating its rapid consumption. In addition, oligomerization and functionalization dominated in both GUA+DMB and GUA+VL, as reported in similar studies (Yu et al., 2014, 2016; Chen et al., 2020; Jiang et al., 2021; Misovich et al., 2021; Mabato et al., 2022). However, functionalization was more prominent in the latter, attributable to the transformation of VL. Nonetheless, it must be noted that for phenolic aqSOA, fragmentation will ultimately be more predominant at longer irradiation times (Huang et al., 2018; Yu et al., 2016; Mabato et al., 2022).

3.1.3 Light absorption of aqSOA from photosensitization by ^{3}DMB* and ^{3}VL*

The absorbance enhancement of phenolic aqSOA generated via reactions with ^{3}DMB*/^{3}VL* has been linked to the formation of conjugated structures due to oligomerization and functionalization (e.g., additions of hydroxyl and carbonyl groups; Yu et al., 2014, 2016; Smith et al., 2016; Chen et al., 2020; Jiang et al., 2021; Misovich et al., 2021; Mabato et al., 2022). Moreover, the aqueous-phase photo-oxidation of BB emissions can enhance BrC absorbance via the formation of aromatic dimers and functionalized products (Hems et al., 2020). In this work, the absorbance enhancement of GUA+DMB

https://doi.org/10.5194/acp-2022-595
Preprint. Discussion started: 23 August 2022


Atmospheric Chemistry and Physics Discussions

and GUA+VL (Fig. 4) correlates with oligomers and functionalized monomers, which are the highest contributors to the product signals. Identifying the chromophores responsible for the absorbance enhancement may be beneficial in understanding the impact of aqSOA on the Earth's radiative balance and determining the reactions that affect light absorption by aqSOA (Mabato et al., 2022). However, the detected products did not exhibit distinct peaks in the UHPLC-PDA chromatograms, likely due to the concentration of the chromophores being below the detection limit of PDA. Nevertheless, the higher absorbance enhancement for GUA+DMB than GUA+VL was most likely associated with the higher contribution and normalized abundance (by ~6 times) of oligomers in the former.

Additional information about aqSOA light absorption can be deduced from the plots of the double bond equivalent (DBE) values vs carbon number (n_C) (Lin et al., 2018). Figure S6 shows these plots along with the DBE reference values of fullerene-like hydrocarbons (Lobodin et al., 2012), cata-condensed polycyclic aromatic hydrocarbons (PAHs; Siegmann and Sattler, 2000), and linear conjugated polyenes with a general formula C_xH_{x+2}. The shaded area indicates a sufficient level of conjugation for visible light absorption, and species within this region are potential BrC chromophores. GUA+DMB and GUA+VL aqSOA exhibited a significant overlap in the DBE vs n_C space; nearly all products from both systems, including the high-relative-abundance species, are potential BrC chromophores. GUA+DMB had more oligomeric products with high relative abundance ($n_C \geq 12$ and DBE ≥ 8). For GUA+VL, high-relative-abundance products also include monomeric species (n_C = 7-8 and 4-5 DBE) corresponding to hydroxylated products (e.g., $C_7H_8O_4$ and $C_8H_8O_5$; 28 and 35; Table S2). These observations further indicate the importance of oligomerization and functionalization for the absorbance enhancement of aqSOA generated via photosensitization by ^{3}DMB* and ^{3}VL*. In summary, ^{3}DMB* and ^{3}VL* can oxidize GUA resulting in aqSOA and BrC formation, but GUA+DMB exhibited stronger light absorption. In GUA+VL, the extent of GUA oxidation was limited by significant VL consumption.

3.2 Comparison of photosensitized GUA oxidation by non-phenolic (^{3}DMB*) and phenolic (^{3}VL*) methoxybenzaldehydes in the presence of AN

3.2.1 Kinetic analysis of photosensitization by ^{3}DMB* and ^{3}VL* in the presence of AN

Ammonium nitrate (AN) did not significantly affect ($p>0.05$) the decay rate constants of GUA, DMB, and VL for both GUA+DMB+AN and GUA+VL+AN (Table 1), likely due to the higher molar absorptivities of the photosensitizers compared to that of nitrate. This implies that the chemistry of ^{3}DMB* and ^{3}VL* dominated that of nitrate. In this work, the GUA decay rate constants decreased in the order of GUA+DMB/GUA+DMB+AN > GUA+VL/GUA+VL+AN > GUA+AN (Table 1). Note that as the molar absorptivities of the photosensitizers are higher than that of nitrate, the kinetics data were also analyzed on a per-photon-absorbed basis for a more appropriate comparison of reaction efficiency (Sect. S6). The apparent quantum efficiency of GUA photodegradation (φ_{GUA}) in the presence of nitrate (GUA+AN: $1.3 \times 10^{-2} \pm 2.9 \times 10^{-3}$) was ~2 and ~7 times higher than that in the presence of DMB ($6.6 \times 10^{-3} \pm 1.9 \times 10^{-4}$) or VL ($1.8 \times 10^{-3} \pm 4.9 \times 10^{-4}$), respectively. This suggests that nitrate-mediated GUA photo-oxidation is more efficient than photosensitization by ^{3}DMB* or ^{3}VL* on a per-photon-absorbed basis.

https://doi.org/10.5194/acp-2022-595
Preprint. Discussion started: 23 August 2022

Atmospheric Chemistry and Physics Discussions

3.2.2 Product distributions and chemical characteristics of aqSOA from photosensitization by ^{3}DMB* and ^{3}VL* in the presence of AN

For both GUA+DMB+AN and GUA+VL+AN, AN had no significant effect on the normalized product abundance (Table 1), but it induced the formation of N-containing products composed of N-heterocycles (e.g., imidazoles and pyridines) and oligomers, as well as nitrated species. Similarly, we previously reported a potential imidazole derivative from the direct photosensitized oxidation of VL in the presence of AN, which was attributed to the reaction of ring-opening products with dissolved ammonia (Mabato et al., 2022). Oligomers remained the highest signal contributors in the presence of AN (Fig. 2), but interactions between photosensitization by ^{3}DMB* and ^{3}VL* and AN photolysis were distinct. First, nitrated species had similar contributions in both cases, but the contribution and normalized abundance of all N-containing products in GUA+DMB+AN were 2 and ~14 times higher, respectively, than in GUA+VL+AN. This difference can be attributed to the higher contribution of N-heterocycles and N-containing oligomers in GUA+DMB+AN. Compared to GUA+VL, GUA+DMB had a higher contribution of ring-opening products which can react with ammonia, as discussed earlier (Figs. 2 and 3). Second, the decrease in oligomers in GUA+DMB+AN may be due to their fragmentation induced by $^{\bullet}$OH from nitrate photolysis, then conversion to N-containing products. Correspondingly, the contribution of possibly ring-retaining N-containing products in GUA+DMB+AN (18.6%) was ~3 times higher than that in GUA+VL+AN (6.5%). While fragmentation of oligomers likely occurred in GUA+VL+AN as well, the increase in oligomers suggests that other reactions have taken place. For GUA+VL+AN, $^{\bullet}$OH or $^{\bullet}NO_2$ from nitrate photolysis may have initiated H-atom abstraction from the –OH group of VL, generating phenoxy radicals which can undergo coupling to form more oligomers (Kobayashi and Higashimura, 2003; Sun et al., 2010; Mabato et al., 2022). This may also explain the more significant decrease of monomers in GUA+VL+AN (~3 times) compared to GUA+DMB+AN (~2 times). Similarly, we previously observed an increase in oligomers upon adding 1 mM AN to 0.01 mM VL (Mabato et al., 2022), the [VL] used in this work. These findings indicate that photosensitization by non-phenolic and phenolic methoxybenzaldehydes may interact differently with AN photolysis.

GUA+AN mainly formed oligomers analogous to $^{\bullet}$OH-mediated phenol oxidation (Yu et al., 2014, 2016), followed by N-containing products. The normalized product abundance of GUA+AN was the lowest among all experiments, likely due to the lower GUA decay constant relative to photosensitized oxidation. Moreover, the normalized abundance of N-containing products in GUA+AN was ~12 times lower than that in GUA+DMB+AN but comparable to that in GUA+VL+AN. This discrepancy for GUA+VL+AN might be due to the weaker signals of its N-containing products in the positive compared to the negative ion mode. As previously mentioned, the normalized product abundance was calculated using only the positive ion mode data as the GUA signal from the negative ion mode was weak and thus may present large uncertainties during normalization. Interestingly, the contributions from nitrated species in GUA+DMB+AN and GUA+VL+AN were higher than in GUA+AN, suggesting possible enhancement of nitration reactions. This is likely due to the increased formation of $^{\bullet}NO_2$, for instance, via the reactions of $^{\bullet}$OH and $O_2^{\bullet-}$ (from ^{3}DMB* or ^{3}VL*) with NO_2^- (Pang et al., 2019; Mabato et al., 2022). This implies that photosensitized reactions may promote reactions induced by nitrate photolysis.

https://doi.org/10.5194/acp-2022-595
Preprint. Discussion started: 23 August 2022


Atmospheric Chemistry and Physics Discussions

The major products from GUA+DMB+AN, GUA+VL+AN, and GUA+AN (Tables S3–S5) include oligomers and functionalized monomers detected in GUA+DMB and GUA+VL (Tables S1–S2). The N-heterocycles from GUA+DMB+AN include $C_6H_6N_4$ (#41; Table S3), which may be 2,2'-biimidazole (BI), a reaction product from glyoxal + reduced nitrogenous compounds (e.g., ammonium salts) (De Haan et al., 2009; Galloway et al., 2009; Nozière et al., 2009; Shapiro et al., 2009; Yu et al., 2011; Kampf et al., 2012; Gen et al., 2018; Mabato et al., 2019). The nitrated products include $C_{12}H_{11}N_3O_3$ and $C_{15}H_{10}N_4O_3$ (#42 and 49; Table S3), which possibly have a nitrated imidazole moiety and a nitrophenol moiety, respectively. For GUA+VL+AN, oligomers ($C_{14}H_{12}O_6$ and $C_{20}H_{16}O_7$; #55 and 59, Table S4) which were not among the major products in GUA+VL were noted. $C_{10}H_8O_2$ has a furanone group (#50; Table S4); furanones are the primary products of the reaction of $^{\bullet}OH$ with toluene and other aromatic hydrocarbons (Smith et al., 1999). Moreover, $C_{11}H_9N_3O_3$ (#57; Table S4) has a nitrated imidazole moiety. Among the N-containing compounds in GUA+AN is $C_4H_3N_3O_3$ (#69; Table S5), which may be a nitrated imidazole-2-carboxaldehyde. Imidazole-2-carboxaldehyde is also a reaction product from glyoxal + reduced nitrogenous compounds (e.g., ammonium salts) (De Haan et al., 2009; Galloway et al., 2009; Nozière et al., 2009; Shapiro et al., 2009; Yu et al., 2011; Kampf et al., 2012; Gen et al., 2018; Mabato et al., 2019).

The ⟨O:C⟩ for GUA+DMB+AN and GUA+VL+AN were lower than those in the absence of AN (Table 1), likely due to the rapid formation of highly oxidized species followed by their decomposition (Huang et al., 2018). The ⟨O:C⟩ and ⟨H:C⟩ were comparable in GUA+DMB+AN and GUA+VL+AN, but the ⟨N:C⟩ for the former was higher, implying a greater extent of reactions involving AN. Relative to GUA+DMB+AN and GUA+VL+AN, GUA+AN had a higher ⟨N:C⟩, as can be expected given that AN was the only oxidant source. The lower $\langle OS_C \rangle$ of GUA+DMB+AN and GUA+VL+AN compared to GUA+AN may be attributed to triplet-initiated oxidation generating higher-molecular-weight products with less fragmentation compared to $^{\bullet}OH$-mediated oxidation (Yu et al., 2014; Chen et al., 2020). Nonetheless, AN generally increased the $\langle OS_C \rangle$ for both GUA+DMB and GUA+VL, with a more noticeable increase for the former, suggesting more oxidized products. Furthermore, GUA+DMB+AN and GUA+VL+AN aqSOA had mainly similar features in the OS_C vs n_C plots as those observed in the absence of AN (Fig. S5). More information on van Krevelen diagrams (Figs. S4e–h and S7) and OS_C vs n_C plots (Figs. S5e–h and S8) for GUA+DMB+AN, GUA+VL+AN, and GUA+AN aqSOA are provided in the Supplement (Sect. S7). In essence, AN had no significant effect on the decay kinetics ascribable to photosensitizer chemistry prevailing over nitrate, but it induced the formation of N-containing products. Moreover, AN modified the product distributions, albeit in different ways (Figs. 2 and 3). In particular, N-containing products were more abundant in GUA+DMB+AN, probably due to more extensive fragmentation in GUA+DMB than in GUA+VL. In GUA+VL+AN, AN promoted oligomer formation likely via the -OH group of VL. Furthermore, GUA+DMB+AN and GUA+VL+AN had more nitrated products than GUA+AN, suggesting that photosensitized reactions may promote nitrate photolysis-initiated reactions.

https://doi.org/10.5194/acp-2022-595
Preprint. Discussion started: 23 August 2022


Atmospheric Chemistry and Physics Discussions

3.2.3 Light absorption of aqSOA from photosensitization by ^{3}DMB* and ^{3}VL* in the presence of AN

The presence of AN also did not appreciably affect the absorbance enhancement for both GUA+DMB+AN and GUA+VL+AN (Fig. 4). For GUA+DMB+AN, the N-containing products may have offset the decrease in oligomers to maintain the absorbance enhancement observed from GUA+DMB. Wang et al. (2022) reported that nitration might contribute significantly to absorbance enhancement for methoxyphenols in sodium nitrate (Wang et al., 2022). In GUA+VL+AN, the decrease in monomers may have counteracted the increased oligomers and generated N-containing products. Compared to GUA+DMB+AN, the N-containing products from GUA+VL+AN probably had less impact on the absorbance enhancement based on their smaller signal contribution.

Similar to experiments without AN, CHO species from GUA+DMB+AN and GUA+VL+AN were mainly overlapped in the DBE vs n_C space (Fig. S6c,d) and were mostly potential BrC chromophores. In both systems, GUA dimers were the products with the highest relative abundance. For GUA+DMB+AN, products with high relative abundance also include a CHN species, while two CHON species had high n_C (18,20) and DBE (16,14) values. In GUA+VL+AN, products with high relative abundance include a CHON species (n_C = 11 and 9 DBE). Approximately 30% and 43% of the N-containing products for GUA+DMB+AN and GUA+VL+AN, respectively, were among the potential BrC chromophores. This suggests the possible significance of N-containing products for light absorption of aqSOA from photosensitization by methoxybenzaldehydes and AN photolysis. Correspondingly, nitroaromatic compounds and N-heterocycles are frequently noted in BBOA (Iinuma et al., 2010; Kitanovski et al., 2012; Kourtchev et al., 2016) and have been proposed to be potential contributors to BrC light absorption (Laskin et al., 2015). Relative to GUA+DMB+AN and GUA+VL+AN, only 19% of the N-containing products in GUA+AN were potential BrC chromophores (Fig. S6e,f), and these did not include CHN species. These indicate that the N-containing products formed in the presence of both photosensitizers and AN may be more significant contributors to the light absorption of phenolic aqSOA than those formed in AN only.

4 Conclusions and atmospheric implications

The photosensitized oxidation of guaiacol (GUA) by triplet excited states of 3,4-dimethoxybenzaldehyde (^{3}DMB*) and vanillin (^{3}VL*) (separately) in the absence and presence of ammonium nitrate (AN) were compared under identical conditions (simulated sunlight and concentration) relevant to atmospheric cloud and fog waters. Compared to GUA+VL, faster GUA oxidation and stronger light absorption were observed in GUA+DMB. Moreover, VL was consumed faster relative to DMB, limiting the extent of GUA oxidation in GUA+VL. These differences are rooted in DMB having a better photosensitizing ability than VL and the –OH group of VL, making it more susceptible to oxidation and more reactive towards electrophilic aromatic substitution. Both GUA+DMB and GUA+VL generated aqSOA, including potential BrC chromophores composed of oligomers, functionalized monomers, oxygenated ring-opening products, and N-containing products in the presence of AN. The major aqSOA formation processes for GUA+DMB and GUA+VL were oligomerization and functionalization, but functionalization appeared to be more significant in GUA+VL due to VL transformation products.

https://doi.org/10.5194/acp-2022-595
Preprint. Discussion started: 23 August 2022


Atmospheric Chemistry and Physics Discussions

AN did not significantly affect the decay kinetics due to the predominant effect of ^{3}DMB* and ^{3}VL* chemistry compared to nitrate, but it promoted the formation of N-containing products; these are composed of N-heterocycles (e.g., imidazoles) and oligomers and nitrated species. The observation of N-heterocycles agrees with our previous findings that ammonium participates in photosensitized oxidation of phenolic compounds in the presence of AN (Mabato et al., 2022). These results also suggest that photosensitized oxidation of phenolic compounds in the presence of AN might be an important source of N-heterocycles and nitrated products. Identifying the sources of N-heterocycles and nitrated compounds is important due to their environmental and health impacts (Laskin et al., 2009). Moreover, photosensitized reactions by non-phenolic and phenolic methoxybenzaldehydes may be differently influenced by AN photolysis. For instance, the more extensive fragmentation in GUA+DMB than in GUA+VL possibly resulted in more N-containing products in GUA+DMB+AN. Furthermore, the increased oligomers in GUA+VL+AN may be due to VL-derived phenoxy radicals induced by $^{\bullet}$OH or $^{\bullet}NO_2$ from nitrate photolysis. In addition, more nitrated compounds observed in GUA+DMB+AN and GUA+VL+AN than in GUA+AN imply that photosensitized reactions may promote nitrate-mediated photolytic reactions. On a related note, the significance of photosensitization by BrC (via formation of solvated electrons; Wang et al., 2021) and marine dissolved organic matter (via $O_2^{\bullet-}$ formation; Garcia et al., 2021) in enhanced nitrite production from nitrate photolysis have been reported. A recent study from our group has shown that glyoxal photo-oxidation mediated by both nitrate photolysis and photosensitization can significantly enhance the atmospheric sink of glyoxal (Zhang et al., 2022). Further studies are needed to improve our understanding of the interplay between photosensitized reactions and nitrate photolysis.

This study demonstrates that the structural features of photosensitizers affect aqSOA formation via non-carbonyl phenol oxidation. The VL results are broadly relevant to other phenolic carbonyls, but the effects of different functional groups should still be considered. For instance, the aldehyde/ketone pair of syringaldehyde and acetosyringone, both phenolic carbonyls, have been reported to have equal reactivity towards direct photosensitized oxidation. This is due to the greater light absorption by the aldehyde form but higher quantum efficiency for loss for the ketone form (Smith et al. 2016). However, more aqSOA was observed from syringaldehyde than acetosyringone (in either AN or ammonium sulfate; Huang et al., 2018). Our findings also imply that while the contributions of photosensitization by ^{3}VL* (and other phenolic carbonyls) to aqSOA formation would be relatively less compared to that of ^{3}DMB* (and other non-phenolic carbonyls), these are not negligible. As both non-phenolic and phenolic carbonyls such as the methoxybenzaldehydes examined in this work are emitted in large amounts from biomass burning, future experiments should probe the aqSOA contribution of a wider variety of photosensitizers. Moreover, further experiments on photosensitized reactions in authentic particulate matter (PM) samples should be conducted in the future. Multicomponent reactions such as GUA+DMB+AN and GUA+VL+AN should also be explored for a more accurate simulation of ambient conditions. These would be useful in assessing the overall impact of photosensitized reactions and AN photolysis on aqSOA formation in areas impacted by biomass burning and high AN concentrations, and for their better representation in aqSOA models.

Data availability.

The data used in this publication are available to the community and can be accessed by request to the corresponding author.

Author contributions.

BRGM designed and conducted the experiments; BRGM and CKC wrote the paper. All co-authors contributed to the discussion of the manuscript.

Competing interests.

The authors declare that they have no conflict of interest.

Acknowledgments.

C.K.C. gratefully acknowledges support from the National Natural Science Foundation of China (42075100 and 41875142) and Hong Kong Research Grants Council (11304121). Y.J.L. acknowledges funding support from the Science and Technology Development Fund, Macau SAR (File No. 0019/2020/A1), and a multiyear research grant (No. MYRG2018-00006-FST) from the University of Macau. The authors also thank the University Research Facility in Chemical and Environmental Analysis (UCEA) at The Hong Kong Polytechnic University for the use of its UHPLC-HESI-Orbitrap Mass Spectrometer and Dr Sirius Tse and Dr Chi Hang Chow for assistance with sample analyses.

References

Anastasio, C., Faust, B. C., and Rao, C. J.: Aromatic carbonyl compounds as aqueous-phase photochemical sources of hydrogen peroxide in acidic sulfate aerosols, fogs, and clouds. 1. Non-phenolic methoxybenzaldehydes and methoxyacetophenones with reductants (phenols), Environ. Sci. Technol., 31, 218−232, https://doi.org/10.1021/es960359g, 1997.

Bateman, A. P., Laskin, J., Laskin, A., and Nizkorodov, S. A.: Applications of high-resolution electrospray ionization mass spectrometry to measurements of average oxygen to carbon ratios in secondary organic aerosols, Environ. Sci. Technol., 46, 8315–832, https://doi.org/10.1021/es3017254, 2012.

Bianco, A., Passananti, M., Brigante, M., and Mailhot, G.: Photochemistry of the cloud aqueous phase: a review, Molecules, 25, 423, https://doi.org/10.3390/molecules25020423, 2020.

Calvert, J. G. and Madronich, S.: Theoretical study of the initial products of the atmospheric oxidation of hydrocarbons, J. Geophys. Res., 92, 2211−2220, https://doi.org/10.1029/JD092iD02p02211, 1987.

Chen, Y., Li, N., Li, X., Tao, Y., Luo, S., Zhao, Z., Ma, S., Huang, H., Chen, Y., Ye, Z., and Ge, X.: Secondary organic aerosol formation from $^{3}C^{*}$-initiated oxidation of 4-ethylguaiacol in atmospheric aqueous-phase, Sci. Total Environ., 723, 137953, https://doi.org/10.1016/j.scitotenv.2020.137953, 2020.

Chen, Z. and Anastasio, C.: Concentrations of a triplet excited state are enhanced in illuminated ice, Environ. Sci.: Processes Impacts, 19, 12−21, https://doi.org/10.1039/C6EM00534A, 2017.

Collett, J. L. Jr., Hoag, K. J., Sherman, D. E., Bator, A., and Richards, L. W.: Spatial and temporal variations in San Joaquin Valley fog chemistry, Atmos. Environ., 33, 129−140, https://doi.org/10.1016/S1352-2310(98)00136-8, 1998.

De Haan, D. O., Hawkins, L. N., Kononenko, J. A., Turley, J. J., Corrigan, A. L., Tolbert, M. A., and Jimenez, J. L.: Formation of nitrogen-containing oligomers by methylglyoxal and amines in simulated evaporating cloud droplets, Environ. Sci. Technol., 45, 984−991, https://doi.org/10.1021/es102933x, 2011.

De Haan, D. O., Pajunoja, A., Hawkins, L. N., Welsh, H. G., Jimenez, N. G., De Loera, A., Zauscher, M., Andretta, A. D., Joyce, B. W., De Haan, A. C., Riva, M., Cui, T., Surratt, J. D., Cazaunau, M., Formenti, P., Gratien, A., Pangui, E., and Doussin, J-F.: Methylamine's effects on methylglyoxal-containing aerosol: chemical, physical, and optical changes, ACS Earth Space Chem., 3, 1706–1716, https://doi.org/10.1021/acsearthspacechem.9b00103, 2019.

De Haan, D. O., Tolbert, M. A., and Jimenez, J. L.: Atmospheric condensed-phase reactions of glyoxal with methylamine, Geophys. Res. Lett., 36, No. L11819, https://doi.org/10.1029/2009GL037441, 2009.

Du, Y., Fu, Q. S., Li, Y., and Su, Y.: Photodecomposition of 4-chlorophenol by reactive oxygen species in UV/air system, J. Hazard. Mater., 186, 491–496, https://doi.org/10.1016/j.jhazmat.2010.11.023, 2011.

Edye, L. A. and Richards, G. N.: Analysis of condensates from wood smoke. components derived from polysaccharides and lignins, Environ. Sci. Technol., 25, 1133−1137, https://doi.org/10.1021/es00018a018, 1991.

Felber, T., Schaefer, T., He, L., and Herrmann, H.: Aromatic carbonyl and nitro compounds as photosensitizers and their photophysical properties in the tropospheric aqueous phase, J. Phys. Chem. A, 125, 5078−5095, https://doi.org/10.1021/acs.jpca.1c03503, 2021.

Galloway, M. M., Chhabra, P. S., Chan, A. W. H., Surratt, J. D., Flagan, R. C., Seinfeld, J. H., and Keutsch, F. N.: Glyoxal uptake on ammonium sulphate seed aerosol: reaction products and reversibility of uptake under dark and irradiated conditions, Atmos. Chem. Phys., 9, 3331–3345, https://doi.org/10.5194/acp-9-3331-2009, 2009.

Garcia, S. L. M., Pandit, S., Navea, J. G., and Grassian, V. H.: Nitrous acid (HONO) formation from the irradiation of aqueous nitrate solutions in the presence of marine chromophoric dissolved organic matter: comparison to other organic photosensitizers, ACS Earth Space Chem., 5, 3056−3064, https://doi.org/10.1021/acsearthspacechem.1c00292, 2021.

Gen, M., Huang, D. D., and Chan, C. K.: Reactive uptake of glyoxal by ammonium-containing salt particles as a function of relative humidity, Environ. Sci. Technol., 52, 6903−6911, https://doi.org/10.1021/acs.est.8b00606, 2018.

Gen, M., Zhang, R., Huang, D. D., Li, Y. J., and Chan, C. K.: Heterogeneous SO_2 oxidation in sulfate formation by photolysis of particulate nitrate, Environ. Sci. Technol. Lett., 6, 86–91, https://doi.org/10.1021/acs.estlett.8b00681, 2019a.

Gen, M., Zhang, R., Huang, D. D., Li, Y. J., and Chan, C. K.: Heterogeneous oxidation of SO_2 in sulfate production during nitrate photolysis at 300 nm: effect of pH, relative humidity, irradiation intensity, and the presence of organic compounds, Environ. Sci. Technol., 53, 8757–8766, https://doi.org/10.1021/acs.est.9b01623, 2019b.

Gen, M., Liang, Z., Zhang, R., Mabato, B. R. G., and Chan, C. K.: Particulate nitrate photolysis in the atmosphere, Environ. Sci.: Atmos., 2, 111–127, https://doi.org/10.1039/d1ea00087j, 2022.

George, C., Brüggemann, M., Hayeck, N., Tinel, L., and Donaldson, J.: Interfacial photochemistry: physical chemistry of gas-liquid interfaces, in: Developments in Physical & Theoretical Chemistry, edited by: Faust, J. A. and House, J. E., Elsevier, 435–457, https://doi.org/10.1016/B978-0-12-813641-6.00014-5, 2018.

Giulianelli, L., Gilardoni, S., Tarozzi, L., Rinaldi, M., Decesari, S., Carbone, C., Facchini, M. C., and Fuzzi, S.: Fog occurrence and chemical composition in the Po valley over the last twenty years, Atmos. Environ., 98, 394–401, https://doi.org/10.1016/j.atmosenv.2014.08.080, 2014.

508 Grace, D. N., Sharp, J. R., Holappa, R. E., Lugos, E. N., Sebold, M. B., Griffith, D. R., Hendrickson, H. P., and, Galloway,
509 M. M.: Heterocyclic product formation in aqueous brown carbon systems, ACS Earth Space Chem., 3, 2472−2481,
510 https://doi.org/10.1021/acsearthspacechem.9b00235, 2019.
511
512 Hawthorne, S. B., Miller, D. J., Langenfeld, J. J., and Krieger, M. S.: PM-10 High-volume collection and quantitation of
513 semi- and nonvolatile phenols, methoxylated phenols, alkanes, and polycyclic aromatic hydrocarbons from winter urban air
514 and their relationship to wood smoke emissions, Environ. Sci. Technol., 26, 2251−2262,
515 https://doi.org/10.1021/es00035a026, 1992.
516
517 Hems, R. F., Schnitzler, E. G., Bastawrous, M., Soong, R., Simpson, A. J., and Abbatt, J. P. D.: Aqueous photoreactions of
518 wood smoke brown carbon, ACS Earth Space Chem., 4, 1149−1160, https://doi.org/10.1021/acsearthspacechem.0c0011,
519 2020.
520
521 Hoshino, M., Akimoto, H., and Okuda, M.: Photochemical oxidation of benzene, toluene, and ethylbenzene initiated by OH
522 radicals in the gas phase, Bull. Chem. Soc. Jpn., 51, 718−724, https://doi.org/10.1246/bcsj.51.718, 1978.
523
524 Huang, D. D., Zhang, Q., Cheung, H. H. Y., Yu, L., Zhou, S., Anastasio, C., Smith, J. D., and Chan, C. K.: Formation and
525 evolution of aqSOA from aqueous-phase reactions of phenolic carbonyls: comparison between ammonium sulfate and
526 ammonium nitrate solutions, Environ. Sci. Technol., 52, 9215–9224, https://doi.org/10.1021/acs.est.8b03441, 2018.
527
528 Iinuma, Y., Böge, O., Gräfe, R., and Herrmann, H.: Methyl-nitrocatechols: atmospheric tracer compounds for biomass
529 burning secondary organic aerosols, Environ. Sci. Technol., 44, 8453–8459, https://doi.org/10.1021/es102938a, 2010.
530
531 Jiang, W., Misovich, M. V., Hettiyadura, A. P. S., Laskin, A., McFall, A. S., Anastasio, C., and Zhang, Q.: Photosensitized
532 reactions of a phenolic carbonyl from wood combustion in the aqueous phase—chemical evolution and light absorption
533 properties of aqSOA, Environ. Sci. Technol., 55, 5199−5211, https://doi.org/10.1021/acs.est.0c07581, 2021.
534
535 Kampf, C. J., Jakob, R., and Hoffmann, T.: Identification and characterization of aging products in the glyoxal/ammonium
536 sulfate system – implications for light-absorbing material in atmospheric aerosols, Atmos. Chem. Phys., 12, 6323–6333,
537 https://doi.org/10.5194/acp-12-6323-2012, 2012.
538
539 Kitanovski, Z., Grgić, I., Vermeylen, R., Claeys, M., and Maenhaut, W.: Liquid chromatography tandem mass spectrometry
540 method for characterization of monoaromatic nitro-compounds in atmospheric particulate matter, J. Chromatogr. A, 1268,
541 35–43, https://doi.org/10.1016/j.chroma.2012.10.021, 2012.
542
543 Kobayashi, S. and Higashimura, H.: Oxidative polymerization of phenols revisited, Prog. Polym. Sci., 28, 1015–1048,
544 https://doi.org/10.1016/S0079-6700(03)00014-5, 2003.
545
546 Kourtchev, I., Fuller, S. J., Giorio, C., Healy, R. M., Wilson, E., O'Connor, I., Wenger, J. C., McLeod, M., Aalto, J.,
547 Ruuskanen, T. M., Maenhaut, W., Jones, R., Venables, D. S., Sodeau, J. R., Kulmala, M., and Kalberer, M.: Molecular
548 composition of biogenic secondary organic aerosols using ultrahigh-resolution mass spectrometry: comparing laboratory and
549 field studies, Atmos. Chem. Phys., 14, 2155−2167, https://doi.org/10.5194/acp-14-2155-2014, 2014.
550
551 Kourtchev, I., Godoi, R. H. M., Connors, S., Levine, J. G., Archibald, A. T., Godoi, A. F. L., Paralovo, S. L., Barbosa, C. G.
552 G., Souza, R. A. F., Manzi, A. O., Seco, R., Sjostedt, S., Park, J., Guenther, A., Kim, S., Smith, J., Martin, S. T., and
553 Kalberer, M.: Molecular composition of organic aerosols in central Amazonia: an ultra-high-resolution mass spectrometry
554 study, Atmos. Chem. Phys., 16, 11899–11913, https://doi.org/10.5194/acp-16-11899-2016, 2016.
555
556 Kroll, J. H., Donahue, N. M., Jimenez, J. L., Kessler, S. H., Canagaratna, M. R., Wilson, K. R., Altieri, K. E., Mazzoleni, L.
557 R., Wozniak, A. S., Bluhm, H., Mysak, E. R., Smith, J. D., Kolb, C. E., and Worsnop, D. R.: Carbon oxidation state as a

558 metric for describing the chemistry of atmospheric organic aerosol, Nat. Chem., 3, 133–139,
559 https://doi.org/10.1038/nchem.948, 2011.
560
561 Laskin, A., Smith, J. S., and Laskin, J.: Molecular characterization of nitrogen-containing organic compounds in biomass
562 burning aerosols using high-resolution mass spectrometry, Environ. Sci. Technol., 43, 3764–3771,
563 https://doi.org/10.1021/es803456n, 2009.
564
565 Laskin, A., Laskin, J., and Nizkorodov, S. A.: Chemistry of atmospheric brown carbon, Chem. Rev., 115, 4335–4382,
566 https://doi.org/10.1021/cr5006167, 2015.
567
568 Laskin, J., Laskin, A., Nizkorodov, S. A., Roach, P., Eckert, P., Gilles, M. K., Wang, B., Lee, H. J., and Hu, Q.: Molecular
569 selectivity of brown carbon chromophores, Environ. Sci. Technol., 48, 12047–12055, https://doi.org/10.1021/es503432r,
570 2014.
571
572 Lee, A. K. Y., Zhao, R., Li, R., Liggio, J., Li, S., and Abbatt, J. P. D.: Formation of light absorbing organo-nitrogen species
573 from evaporation of droplets containing glyoxal and ammonium sulfate, Environ. Sci. Technol., 47, 12819−12826,
574 https://doi.org/10.1021/es402687w, 2013.
575
576 Li, P., Li, X., Yang, C., Wang, X., Chen, J., and Collett, J. L. Jr.: Fog water chemistry in Shanghai, Atmos. Environ., 45,
577 4034−4041, https://doi.org/10.1016/j.atmosenv.2011.04.036, 2011.
578
579 Li, Y. J., Huang, D. D., Cheung, H. Y., Lee, A. K. Y., and Chan, C. K.: Aqueous-phase photochemical oxidation and direct
580 photolysis of vanillin - a model compound of methoxy phenols from biomass burning, Atmos. Chem. Phys., 14, 2871−2885,
581 https://doi.org/10.5194/acp-14-2871-2014, 2014.
582
583 Liang, Z., Zhang, R., Gen, M., Chu, Y., and Chan, C. K.: Nitrate photolysis in mixed sucrose–nitrate–sulfate particles at
584 different relative humidities, J. Phys. Chem. A, 125, 3739–3747, https://doi.org/10.1021/acs.jpca.1c00669, 2021.
585
586 Lin, P., Yu, J. Z., Engling, G., and Kalberer, M.: Organosulfates in humic-like substance fraction isolated from aerosols at
587 seven locations in East Asia: a study by ultra-high-resolution mass spectrometry, Environ. Sci. Technol., 46, 13118–13127,
588 https://doi.org/10.1021/es303570v, 2012.
589
590 Lin, P., Fleming, L. T., Nizkorodov, S. A., Laskin, J., and Laskin, A.: Comprehensive molecular characterization of
591 atmospheric brown carbon by high resolution mass spectrometry with electrospray and atmospheric pressure
592 photoionization, Anal. Chem., 90, 12493–12502, https://doi.org/10.1021/acs.analchem.8b02177, 2018.
593
594 Lipari, F., Dasch, J. M., and Scruggs, W. F.: Aldehyde emissions from wood-burning fireplaces, Environ. Sci. Technol., 18,
595 326−330, https://doi.org/10.1021/es00123a007, 1984.
596
597 Liu, C., Chen, D., and Chen, X.: Atmospheric reactivity of methoxyphenols: a review, Environ. Sci. Technol., 56, 2897–
598 2916, https://doi.org/10.1021/acs.est.1c06535, 2022.
599
600 Lobodin, V. V., Marshall, A. G., and Hsu, C. S.: Compositional space boundaries for organic compounds, Anal. Chem., 84,
601 3410–3416, https://doi.org/10.1021/ac300244f, 2012.
602
603 Mabato, B. R. G., Gen, M., Chu, Y., and Chan, C. K.: Reactive uptake of glyoxal by methylaminium-containing salts as a
604 function of relative humidity, ACS Earth Space Chem., 3, 150–157, https://doi.org/10.1021/acsearthspacechem.8b00154,
605 2019.

https://doi.org/10.5194/acp-2022-595
Preprint. Discussion started: 23 August 2022

Atmospheric Chemistry and Physics Discussions

606 Mabato, B. R. G., Lyu, Y., Ji, Y., Li, Y. J., Huang, D. D., Li, X., Nah, T., Lam, C. H., and Chan, C. K.: Aqueous secondary
607 organic aerosol formation from the direct photosensitized oxidation of vanillin in the absence and presence of ammonium
608 nitrate, Atmos. Chem. Phys., 22, 273−293, https://doi.org/10.5194/acp-22-273-2022, 2022.
609
610 Mazzoleni, L. R., Saranjampour, P., Dalbec, M. M., Samburova, V., Hallar, A. G., Zielinska, B., Lowenthal, D. H., and
611 Kohl, S.: Identification of water-soluble organic carbon in non-urban aerosols using ultrahigh-resolution FT-ICR mass
612 spectrometry: organic anions, Environ. Chem., 9, 285−297, https://doi.org/10.1071/EN11167, 2012.
613
614 Minero, C., Bono, F., Rubertelli, F., Pavino, D., Maurino, V., Pelizzetti, E., and Vione, D.: On the effect of pH in aromatic
615 photonitration upon nitrate photolysis, Chemosphere, 66, 650−656, https://doi.org/10.1016/j.chemosphere.2006.07.082, 2007.
616
617 Misovich, M. V., Hettiyadura, A. P. S., Jiang, W., Zhang, Q., and Laskin, A.: Molecular-level study of the photo-oxidation
618 of aqueous-phase guaiacyl acetone in the presence of $^{3}C^{*}$: formation of brown carbon products, ACS Earth Space Chem., 5,
619 1983−1996, https://doi.org/10.1021/acsearthspacechem.1c00103, 2021.
620
621 Munger, J. W., Jacob, D. J., Waldman, J. M., and Hoffmann, M. R.: Fogwater chemistry in an urban atmosphere, J.
622 Geophys. Res. [Oceans], 88, 5109–5121, https://doi.org/10.1029/JC088iC09p05109, 1983.
623
624 Nolte, C. G., Schauer, J. J., Cass, G. R., and Simoneit, B. R. T.: Highly polar organic compounds present in wood smoke and
625 in the ambient atmosphere, Environ. Sci. Technol., 35, 1912−1919, https://doi.org/10.1021/es001420r, 2001.
626
627 Nozière, B., Dziedzic, P., and Córdova, A.: Products and kinetics of the liquid-phase reaction of glyoxal catalyzed by
628 ammonium ions (NH_4^+), J. Phys. Chem. A, 113, 231−237, https://doi.org/10.1021/jp8078293, 2009.
629
630 Nozière, B., Dziedzic, P., and Córdova, A.: Inorganic ammonium salts and carbonate salts are efficient catalysts for aldol
631 condensation in atmospheric aerosols, Phys. Chem. Chem. Phys., 12, 3864−3872, https://doi.org/10.1039/B924443C, 2010.
632
633 Nozière, B., Fache, F., Maxut, A., Fenet, B., Baudouin, A., Fine, L., and Ferronato, C.: The hydrolysis of epoxides catalyzed
634 by inorganic ammonium salts in water: kinetic evidence for hydrogen bond catalysis, Phys. Chem. Chem. Phys., 20,
635 1583−1590, https://doi.org/10.1039/C7CP06790A, 2018.
636
637 Pang, H., Zhang, Q., Lu, X., Li, K., Chen, H., Chen, J., Yang, X., Ma, Y., Ma, J., and Huang, C.: Nitrite-mediated
638 photooxidation of vanillin in the atmospheric aqueous phase, Environ. Sci. Technol., 53, 14253−14263,
639 https://doi.org/10.1021/acs.est.9b03649, 2019.
640
641 Powelson, M. H., Espelien, B. M., Hawkins, L. N., Galloway, M. M., and De Haan, D. O.: Brown carbon formation by
642 aqueous-phase carbonyl compound reactions with amines and ammonium sulfate, Environ. Sci. Technol., 48, 985−993,
643 https://doi.org/10.1021/es4038325, 2014.
644
645 Pye, H. O. T., Nenes, A., Alexander, B., Ault, A. P., Barth, M. C., Clegg, S. L., Collett, J. L. Jr., Fahey, K. M., Hennigan, C.
646 J., Herrmann, H., Kanakidou, M., Kelly, J. T., Ku, I., McNeill, V. F., Riemer, N., Schaefer, T., Shi, G., Tilgner, A., Walker,
647 J. T., Wang, T., Weber, R., Xing, J., Zaveri, R. A., and Zuend, A.: The acidity of atmospheric particles and clouds, Atmos.
648 Chem. Phys., 20, 4809–4888, https://doi.org/10.5194/acp-20-4809-2020, 2020.
649
650 Raja, S., Raghunathan, R., Yu, X., Lee, T., Chen, J., Kommalapati, R. R., Murugesan, K., Shen, X., Qingzhong, Y., Valsaraj,
651 K. T., and Collett, J. L. Jr.: Fog chemistry in the Texas-Louisiana Gulf Coast corridor, Atmos. Environ., 42, 2048−2061,
652 https://doi.org/10.1016/j.atmosenv.2007.12.004, 2008.
653

654 Rogge, W. F., Hildemann, L. M., Mazurek, M. A., and Cass, G. R.: Sources of fine organic aerosol. 9. Pine, oak, and
655 synthetic log combustion in residential fireplaces, Environ. Sci. Technol., 32, 13−22, https://doi.org/10.1021/es960930b,
656 1998.
657
658 Sagebiel, J. C., Seiber, J. N., and Woodrow, J. E.: Comparison of headspace and gas-stripping methods for determining the
659 Henry's law constant (H) for organic compounds of low to intermediate H, Chemosphere, 25, 1763–1768,
660 https://doi.org/10.1016/0045-6535(92)90017-L, 1992.
661
662 Schauer, J. J., Kleeman, M. J., Cass, G. R., and Simoneit, B. R. T.: Measurement of emissions from air pollution sources. 3.
663 C_1-C_{29} organic compounds from fireplace combustion of wood, Environ. Sci. Technol., 35, 1716−1728,
664 https://doi.org/10.1021/es001331e, 2001.
665
666 Shapiro, E. L., Szprengiel, J., Sareen, N., Jen, C. N., Giordano, M. R., and McNeill, V. F.: Light-absorbing secondary
667 organic material formed by glyoxal in aqueous aerosol mimics, Atmos. Chem. Phys., 9, 2289−2300,
668 https://doi.org/10.5194/acp-9-2289-2009, 2009.
669
670 Siegmann, K. and Sattler, K.: Formation mechanism for polycyclic aromatic hydrocarbons in methane flames, J. Chem.
671 Phys., 112, 698–709, https://doi.org/10.1063/1.480648, 2000.
672
673 Simoneit, B. R. T.: Biomass burning — a review of organic tracers for smoke from incomplete combustion, Appl.
674 Geochem., 17, 129–162, https://doi.org/10.1016/S0883-2927(01)00061-0, 2002.
675
676 Simoneit, B. R. T., Rogge, W. F., Mazurek, M. A., Standley, L. J., Hildemann, L. M., and Cass, G. R.: Lignin pyrolysis
677 products, lignans, and resin acids as specific tracers of plant classes in emissions from biomass combustion, Environ. Sci.
678 Technol., 27, 2533−2541, https://doi.org/10.1021/es00048a034, 1993.
679
680 Simoneit, B. R. T., Schauer, J. J., Nolte, C. G., Oros, D. R., Elias, V. O., Fraser, M. P., Rogge, W. F., and Cass, G. R.:
681 Levoglucosan, a tracer for cellulose in biomass burning and atmospheric particles, Atmos. Environ., 33, 173−182,
682 https://doi.org/10.1016/S1352-2310(98)00145-9, 1999.
683
684 Simpson, C. D., Paulsen, M., Dills, R. L., Liu, L.-J. S., and Kalman, D. A.: Determination of methoxyphenols in ambient
685 atmospheric particulate matter: tracers for wood combustion, Environ. Sci. Technol., 39, 631−637,
686 https://doi.org/10.1021/es0486871, 2005.
687
688 Slikboer, S., Grandy, L., Blair, S. L., Nizkorodov, S. A., Smith, R. W., and Al-Abadleh, H. A.: Formation of light absorbing
689 soluble secondary organics and insoluble polymeric particles from the dark reaction of catechol and guaiacol with Fe(III),
690 Environ. Sci. Technol., 49, 7793–7801, https://doi.org/10.1021/acs.est.5b01032, 2015.
691
692 Smith, D. F., Kleindienst, T. E., and McIver, C. D.: Primary product distributions from the reaction of OH with m-, p-xylene,
693 1,2,4-and 1,3,5-trimethylbenzene, J. Atmos. Chem., 34, 339–364, https://doi.org/10.1023/A:1006277328628, 1999.
694
695 Smith, J. D., Sio, V., Yu, L., Zhang, Q., and Anastasio, C.: Secondary organic aerosol production from aqueous reactions of
696 atmospheric phenols with an organic triplet excited state, Environ. Sci. Technol., 48, 1049–1057,
697 https://doi.org/10.1021/es4045715, 2014.
698
699 Smith, J. D., Kinney, H., and Anastasio, C.: Aqueous benzene-diols react with an organic triplet excited state and hydroxyl
700 radical to form secondary organic aerosol, Phys. Chem. Chem. Phys., 17, 10227−10237,
701 https://doi.org/10.1039/C4CP06095D, 2015.
702

Smith, J. D., Kinney, H., and Anastasio, C.: Phenolic carbonyls undergo rapid aqueous photodegradation to form low-volatility, light-absorbing products, Atmos. Environ., 126, 36−44, https://doi.org/10.1016/j.atmosenv.2015.11.035, 2016.

Sun, Y. L., Zhang, Q., Anastasio, C., and Sun, J.: Insights into secondary organic aerosol formed via aqueous-phase reactions of phenolic compounds based on high resolution mass spectrometry, Atmos. Chem. Phys., 10, 4809−4822, https://doi.org/10.5194/acp-10-4809-2010, 2010.

US EPA: Estimation Programs Interface Suite™ for Microsoft® Windows, v 4.1, United States Environmental Protection Agency, Washington, DC, USA, 2012.

Wang, Y., Huang, D. D., Huang, W., Liu, B., Chen, Q., Huang, R., Gen, M., Mabato, B. R. G., Chan, C. K., Li, X., Hao, T., Tan, Y., Hoi, K. I., Mok, K. M., and Li, Y. J.: Enhanced nitrite production from the aqueous photolysis of nitrate in the presence of vanillic acid and implications for the roles of light-absorbing organics, Environ. Sci. Technol., 55, 15694−15704, https://doi.org/10.1021/acs.est.1c04642, 2021.

Wang, Y., Huang, W., Tian, L., Wang, Y., Li, F., Huang, D. D., Zhang, R., Mabato, B. R. G., Huang, R., Chen, Q., Ge, X., Du, L., Ma, Y. G., Gen, M., Hoi, K. I., Mok, K. M., Yu, J. Z., Chan, C. K., Li, X., and Li, Y. J.: Decay kinetics and absorption changes of methoxyphenols and nitrophenols during nitrate-mediated aqueous photochemical oxidation at 254 and 313 nm, ACS Earth Space Chem., 6, 1115−1125, https://doi.org/10.1021/acsearthspacechem.2c00021, 2022.

Yang, J., Au, W. C., Law, H., Leung, C. H., Lam, C. H, and Nah, T.: pH affects the aqueous-phase nitrate-mediated photooxidation of phenolic compounds: implications for brown carbon formation and evolution, Environ. Sci.: Processes Impacts, https://doi.org/10.1039/D2EM00004K, 2022.

Yasmeen, F., Vermeylen, R., Szmigielski, R., Iinuma, Y., Böge, O., Herrmann, H., Maenhaut, W., and Claeys, M.: Terpenylic acid and related compounds: precursors for dimers in secondary organic aerosol from the ozonolysis of α and β-pinene, Atmos. Chem. Phys., 10, 9383–9392, https://doi.org/10.5194/acp-10-9383-2010, 2010.

Yaws, C. L.: Handbook of vapor pressure, volume 3: Organic compounds C8 to C28, Gulf Professional Publishing, 1994.

Ye, Z., Qu, Z., Ma, S., Luo, S., Chen, Y., Chen, H., Chen, Y., Zhao, Z., Chen, M., and Ge, X.: A comprehensive investigation of aqueous-phase photochemical oxidation of 4-ethylphenol, Sci. Total Environ., 685, 976–985, https://doi.org/10.1016/j.scitotenv.2019.06.276, 2019.

Yu, G., Bayer, A. R., Galloway, M. M., Korshavn, K. J., Fry, C. G., and Keutsch, F. N.: Glyoxal in aqueous ammonium sulfate solutions: products, kinetics and hydration effects, Environ. Sci. Technol., 45, 6336−6342, https://doi.org/10.1021/es200989n, 2011.

Yu, L., Smith, J., Laskin, A., Anastasio, C., Laskin, J., and Zhang, Q.: Chemical characterization of SOA formed from aqueous-phase reactions of phenols with the triplet excited state of carbonyl and hydroxyl radical, Atmos. Chem. Phys., 14, 13801−13816, https://doi.org/10.5194/acp-14-13801-2014, 2014.

Yu, L., Smith, J., Laskin, A., George, K. M., Anastasio, C., Laskin, J., Dillner, A. M., and Zhang, Q.: Molecular transformations of phenolic SOA during photochemical aging in the aqueous phase: competition among oligomerization, functionalization, and fragmentation, Atmos. Chem. Phys., 16, 4511−4527, https://doi.org/10.5194/acp-16-4511-2016.

Zhang, Q. and Anastasio, C.: Conversion of fogwater and aerosol organic nitrogen to ammonium, nitrate, and NO_x during exposure to simulated sunlight and ozone, Environ. Sci. Technol., 37, 3522–3530, https://doi.org/10.1021/es034114x, 2003.

https://doi.org/10.5194/acp-2022-595
Preprint. Discussion started: 23 August 2022

Atmospheric Chemistry and Physics Discussions

Zhang, R., Gen, M., Huang, D. D., Li, Y. J., and Chan, C. K.: Enhanced sulfate production by nitrate photolysis in the presence of halide ions in atmospheric particles, Environ. Sci. Technol., 54, 3831–3839, https://doi.org/10.1021/acs.est.9b06445, 2020.

Zhang, R., Gen, M., Fu, T-M., and Chan, C. K.: Production of formate via oxidation of glyoxal promoted by particulate nitrate photolysis, Environ. Sci. Technol., 55, 5711–5720, https://doi.org/10.1021/acs.est.0c0819, 2021.

Zhang, R., Gen, M., Liang, Z., Li, Y. J., and Chan, C. K.: Photochemical reactions of glyoxal during particulate ammonium nitrate photolysis: Brown carbon formation, enhanced glyoxal decay, and organic phase formation, Environ. Sci. Technol., 56, 1605–1614, https://doi.org/10.1021/acs.est.1c07211, 2022.

Zielinski, T., Bolzacchini, E., Cataldi, M., Ferrero, L., Graßl, S., Hansen, G., Mateos, D., Mazzola, M., Neuber, R., Pakszys, P., Posyniak, M., Ritter, C., Severi, M., Sobolewski, P., Traversi, R., and Velasco-Merino, C.: Study of chemical and optical properties of biomass burning aerosols during long-range transport events toward the Arctic in summer 2017, Atmosphere, 11, 84, https://doi.org/10.3390/atmos11010084, 2020.

https://doi.org/10.5194/acp-2022-595
Preprint. Discussion started: 23 August 2022

Atmospheric Chemistry and Physics Discussions

Table 1. Reaction conditions, initial GUA (and DMB or VL) decay rate constants, normalized abundance of products, average elemental ratios, and average carbon oxidation state ($\langle OS_C \rangle$) in each experiment. The reaction systems consisted of GUA (0.1 mM), DMB (0.01 mM), VL (0.01 mM), and AN (1 mM) under air-saturated conditions after 180 min of simulated sunlight irradiation. The UHPLC-HESI-Orbitrap-MS data were obtained in both positive (POS) and negative (NEG) ion modes.

Exp no.	Reaction conditions	Initial GUA (and DMB or VL) decay rate constants (min^{-1})[a]	Normalized abundance of products[b]	Normalized abundance of N-containing compounds[b]	$\langle O:C \rangle^c$	$\langle H:C \rangle^c$	$\langle N:C \rangle^c$	$\langle OS_C \rangle^c$
1	GUA+DMB	GUA: $5.4 \times 10^{-2} \pm 3.0 \times 10^{-4}$ DMB: $6.7 \times 10^{-3} \pm 1.2 \times 10^{-4}$	376 ± 22	NA	POS: 0.34	0.91	NA	-0.22
					NEG: 0.40	0.94	NA	-0.15
2	GUA+ DMB+AN	GUA: $4.8 \times 10^{-2} \pm 6.4 \times 10^{-4}$ DMB: $6.2 \times 10^{-3} \pm 6.5 \times 10^{-5}$	310 ± 4	114	POS: 0.28	0.94	0.12	-0.03
					NEG: 0.37	0.91	0.04	-0.05
3	GUA+VL	GUA: $1.4 \times 10^{-2} \pm 1.8 \times 10^{-4}$ VL: $3.3 \times 10^{-2} \pm 7.0 \times 10^{-4}$	94 ± 5	NA	POS: 0.41	0.91	NA	-0.10
					NEG: 0.40	0.94	NA	-0.14
3	GUA+ VL+AN	GUA: $1.5 \times 10^{-2} \pm 1.6 \times 10^{-4}$ VL: $2.8 \times 10^{-2} \pm 4.9 \times 10^{-5}$	100 ± 2	8	POS: 0.31	1.02	0.02	-0.34
					NEG: 0.39	0.91	0.03	-0.02
5	GUA+AN	$8.1 \times 10^{-3} \pm 7.2 \times 10^{-5}$	23 ± 1	9	POS: 0.35	0.99	0.16	0.19
					NEG: 0.38	1.01	0.05	-0.08

[a]The data fitting was performed in the initial linear region. Each value is the average of results from triplicate experiments. Errors represent one standard deviation. [b]The normalized product abundance was calculated using the data from UHPLC-HESI-Orbitrap-MS in the positive (POS) ion mode as the GUA signal from the negative (NEG) ion mode was weak, which may introduce significant uncertainties during normalization. The uncertainties were propagated from the changes in [GUA] measured using UHPLC-PDA and the MS signal intensities. The samples for experiments without AN (marked with NA) were not analyzed for N-containing compounds. [c]The average elemental ratios ($\langle O:C \rangle$, $\langle H:C \rangle$, and $\langle N:C \rangle$) and $\langle OS_C \rangle$ were based on the UHPLC-HESI-Orbitrap-MS results and estimated using the signal-weighted method (Bateman et al., 2012). The $\langle OS_C \rangle$ of GUA, DMB, and VL are -0.57, -0.44, and -0.25, respectively.

https://doi.org/10.5194/acp-2022-595
Preprint. Discussion started: 23 August 2022

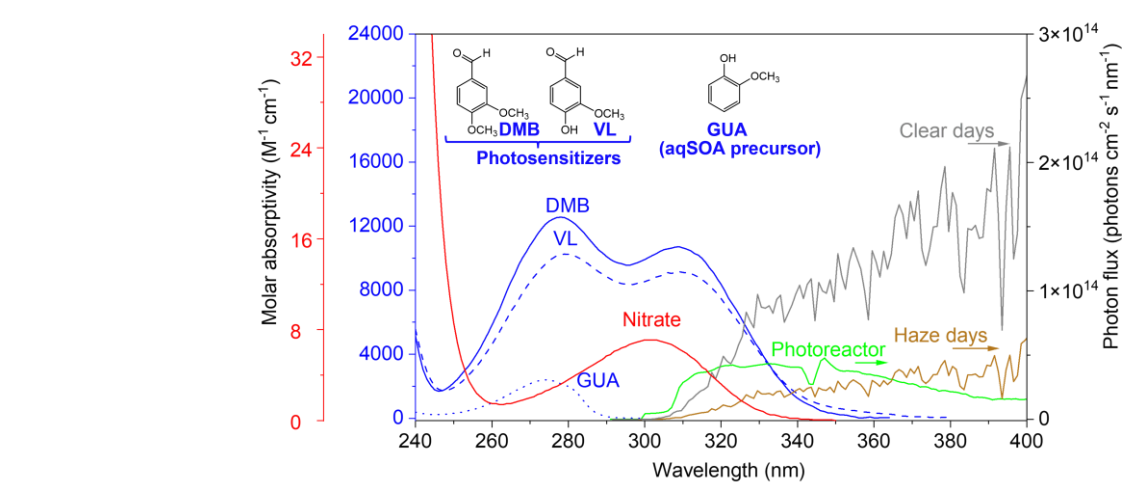

Figure 1. The base-10 molar absorptivities (M^{-1} cm^{-1}) of 3,4-dimethoxybenzaldehyde (DMB, blue solid line), vanillin (VL, blue dashed line), guaiacol (GUA, blue dotted line), and nitrate (red solid line). The green line is the photon flux in the aqueous photoreactor. The gray and brown lines are the photon fluxes on clear or haze days, respectively, in Beijing, China (Mabato et al., 2022). The top of the figure also shows the structures of DMB, VL, and GUA.

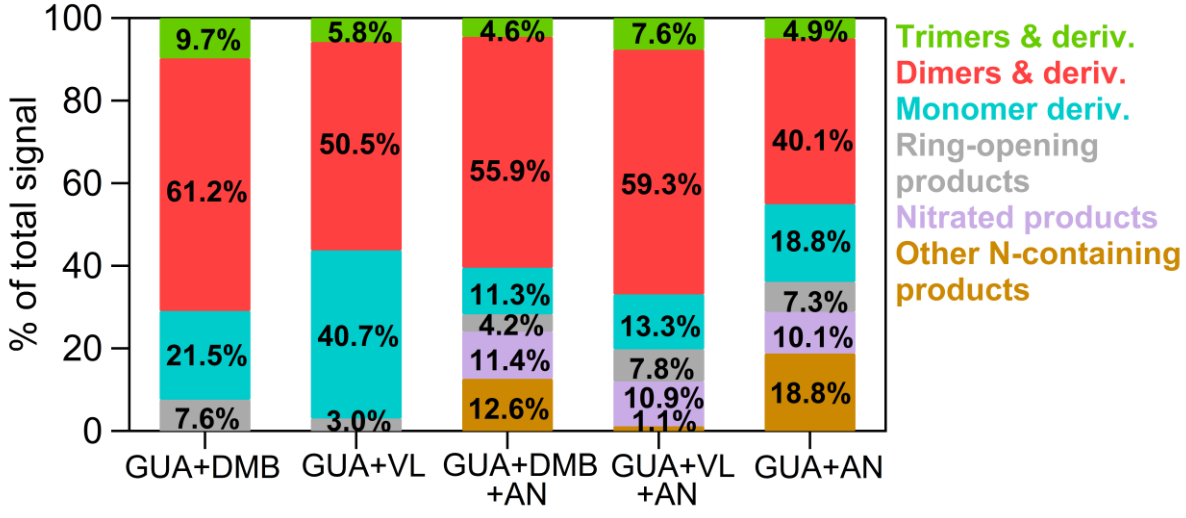

Figure 2. Signal-weighted distributions of aqSOA from GUA+DMB, GUA+VL, GUA+DMB+AN, GUA+VL+AN, and GUA+AN. These product distributions were calculated from combined UHPLC-HESI-Orbitrap-MS data obtained in positive (POS) and negative (NEG) ion modes. The values indicate the contribution of different product classifications to the total signals for each reaction condition.

https://doi.org/10.5194/acp-2022-595
Preprint. Discussion started: 23 August 2022

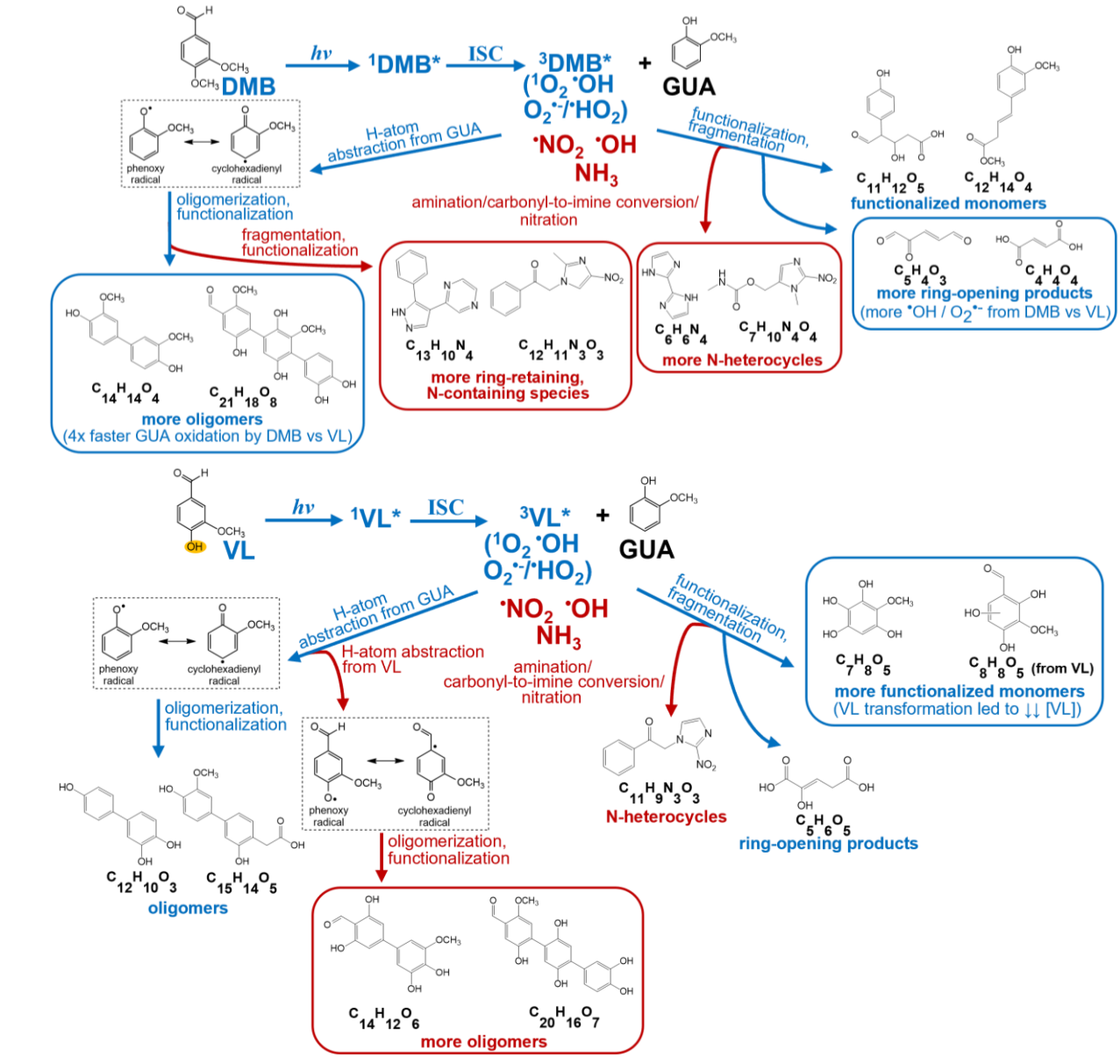

Figure 3. Summary of the main differences between photosensitized GUA oxidation by ^{3}DMB* (top) and ^{3}VL* (bottom) in the absence (blue labels and boxes) and presence (red labels and boxes) of ammonium nitrate at pH 4 under air-saturated conditions. Boxed structures indicate product classifications with notable differences. DMB and VL absorb light and are promoted to their singlet excited states (^{1}DMB* and ^{1}VL*), which then undergo intersystem crossing (ISC) to form ^{3}DMB* and ^{3}VL*. Secondary oxidants ($^1O_2$, $O_2^{\bullet-}$/$^\bullet HO_2$, $^\bullet$OH) can be formed from ^{3}DMB* and ^{3}VL* upon reactions with O_2 and GUA (George et al., 2018; Chen et al., 2020; Misovich et al., 2021; Mabato et al., 2022). The structures shown are examples of the major products (Tables S1 to S4) for different product classifications.

https://doi.org/10.5194/acp-2022-595
Preprint. Discussion started: 23 August 2022

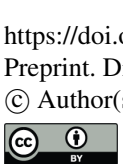

Atmospheric Chemistry and Physics Discussions

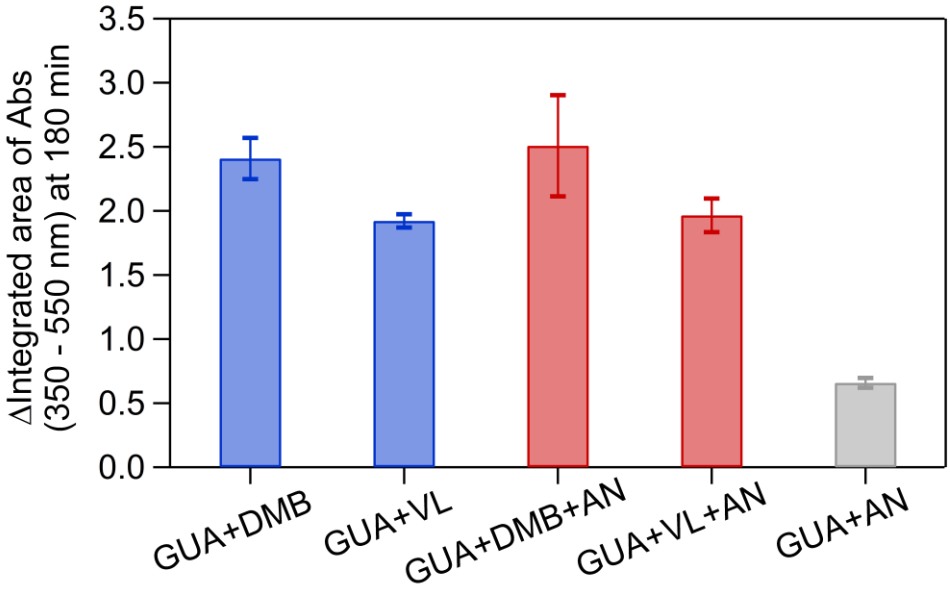

Figure 4. Increase in visible light absorption for aqSOA from GUA+DMB, GUA+VL, GUA+DMB+AN, and GUA+VL+AN. Error bars represent one standard deviation of triplicate experiments.